

*Third European Rotorcraft and Powered-Lift Aircraft Forum*

Paper No. 4

## **The Bearingless Main Rotor**

**Franklin D. Harris**  
Boeing Vertol Company  
Philadelphia, Pennsylvania, USA

**Patrick A. Cancro**  
U.S. Army Air Mobility Research  
and Development Laboratory  
Fort Eustis, Virginia, USA

**Peter G. C. Dixon**  
Boeing Vertol Company  
Philadelphia, Pennsylvania, USA

September 7-9, 1977

*Aix-en-Provence, France*

Association Aeronautique et Astronautique de France





## THE BEARINGLESS MAIN ROTOR

Franklin D. Harris  
Boeing Vertol Company

Patrick A. Cancro  
U.S. Army Air Mobility Research  
and Development Laboratory

Peter G. C. Dixon  
Boeing Vertol Company

### Introduction

The Boeing Vertol Company is presently under contract with the United States Army Air Mobility Research and Development Laboratory to develop and fly a bearingless main rotor on the BO-105 helicopter. The Bearingless Main Rotor (BMR) completes the evolution of rotor hubs from the fully articulated and hingeless rotor hubs. Boeing's work on the bearingless main rotor began as an outgrowth of its bearingless tail rotor developed for the YUH-61A. During 1974 and 1975, conceptual studies led to an attractive BMR concept. In June of 1976 the contract was awarded; the program has since passed through the key steps of preliminary design and is now in the detail design phase.

This paper presents and discusses design features of the configuration. It also presents a thorough discussion of aeroelastic stability results and describes the structural analysis and test results. Finally, a review is given of activities planned from now until flight-test results are available in July 1978.

### Design Features

The Boeing Vertol bearingless main rotor, over a period of nearly five years in development, is now designed as shown in Figure 1. The configuration attaches a modified BO-105 blade to a set of dual fiberglass beams. The blade-to-beam joint is made at the 25-percent radius station. The beam's root end is then pinned at the 2.38-percent radius station to a metal hub-plate set. Blade pitch is controlled by a torque tube. The outboard end of the torque tube is bolted solidly (cantilevered) at the blade-to-beam joint. The torque tube is supported at its inboard end with a rod-end bearing of the type used in helicopter upper control assemblies. The fiberglass beams are made of 3M 1002 SF-1 preimpregnated material and are laid up in matched metal dies. The fiberglass beams have basically a C-channel (  $\square$  ) cross section. All the geometric parameters of

the individual beams such as width, height, flange and web thickness, and spacing between the two beams vary along the 52-inch nominal length. The fiberglass beams permit flapwise bending, chordwise bending, and full torsional travel. The BMR, as designed to fly on the BO-105, has flap, chord, and torsion frequencies at approximately the current BO-105 values; thus, the BMR is a soft-in-plane rotor.

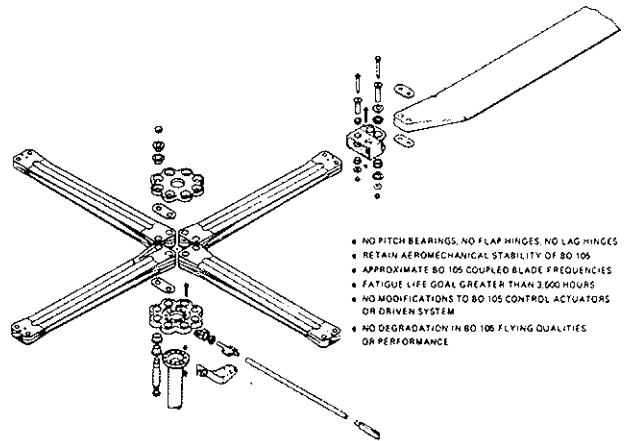


Figure 1. Design Criteria for the Bearingless Main Rotor for the BO-105

The rotor-system natural-frequency diagram is shown in Figure 2. Calculated results indicate that at the operating rpm of 425, the rotating frequencies on a per-rev basis are as follows:

- First flap - 1.119
- Second flap - 2.575
- Third flap - 4.336
- First chord - 0.739 (0.682 desired and expected based on model tests)
- Second chord - 3.854
- Third chord - 8.912
- First torsion - 3.698
- Second torsion - 7.683

Copies of this paper are available from the Technical Library, Boeing Vertol Company, Box 16858, Philadelphia, Pennsylvania, 19142, USA.

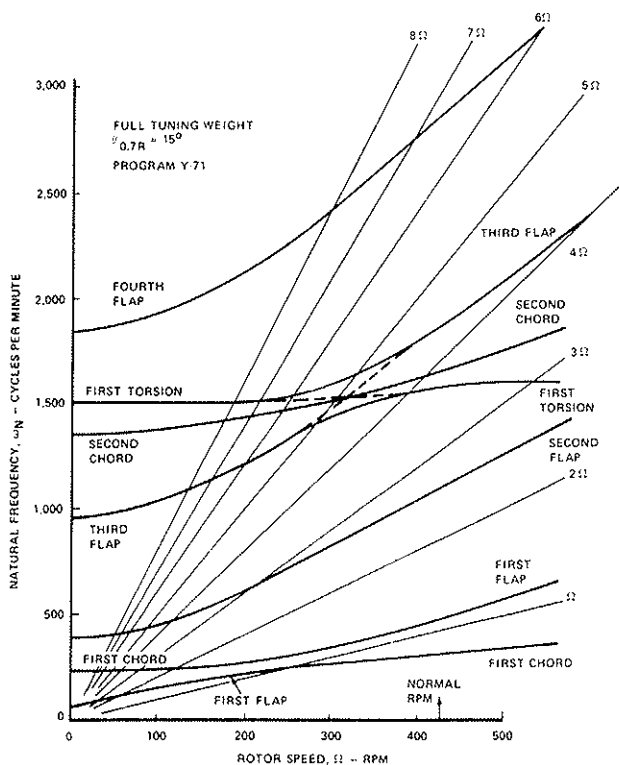


Figure 2. Predicted Fully Coupled Natural Frequencies for the Bearingless Main Rotor System

With respect to these frequencies, the torque tube is nearly 10 times as stiff in torsion as the fiberglass beams themselves. Therefore, the calculated first-torsion frequency at 425 rpm with the torque tube removed approaches 1.3/rev. The torque tube is approximately 1/10 the stiffness of the beams in flap bending and chord bending. Thus, the basic torsional rigidity is set by the torque tube while the fiberglass beams set the flapwise and chordwise frequencies. Secondly, we are purposely designing to a high first-chord frequency of 0.739/rev, in order to achieve the desired value of 0.682/rev. This difference between the calculated first-chord frequency and the experimentally achieved frequency was established based on Froude-scaled model testing.

Aeroelastic Stability Results

As stated in the contractual objective of this program, "It is anticipated that the results of the program will either prove the feasibility of the BMR or indicate what technical inadequacies still exist that need to be resolved." The major question under consideration here is that of air-resonance stability. An early program conducted by Lockheed<sup>1</sup> ended with curtailment of flight test after a few hours of testing because the margins between air and ground resonance in terms of an

operating rpm range were much too small. Therefore, questions dealing with air and ground resonance have received major emphasis in the early phases of this BMR program.

The problem of air and ground resonance can be presented rather simply as shown in Figure 3. Both types of resonance are dominated by rotor-blade lead/lag motion coupling with body motion. As illustrated in Figure 3, the key frequencies of both body and rotor vary with rotor speed. The rotor forcing frequency is the first-chord frequency minus rotor speed. Since the rotor forcing frequency crosses the body frequencies, both air and ground resonance may occur. In the case of the BMR as designed for the BO-105, a wide band in allowable rotor speed is shown in Figure 3. For example, the rotor forcing frequency crosses the body roll in air at approximately 320 rpm and air resonance could be suspected here. With increasing rpm, the rotor forcing frequency crosses the body roll in air at approximately 475 rpm and air resonance could be expected at this point. The possibility of ground resonance could be anticipated because rotor forcing frequency crosses body pitch motion on the ground at 570 rpm. It is these intersections of rotor forcing frequency with the body while in the air or on the ground that have been explored very early in this program.

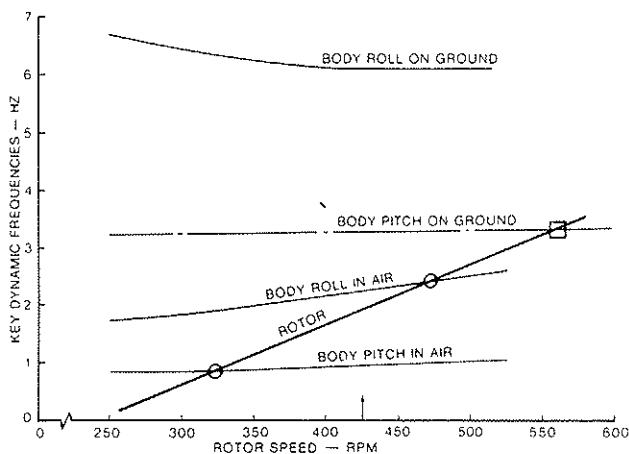


Figure 3. When Rotor Forcing Frequency Comes Close to Body Frequencies, Air and Ground Resonance May Occur

Air Resonance

To complement the air- and ground-resonance theories developed and used on the BMR program<sup>2</sup>, a Froude-scaled air-resonance model as shown in Figure 4 was developed. This 5.5-foot-diameter model has a scale factor of 1/5.86. The model is free to pitch and roll about a two-axis gimbal system. A pilot flies the model with a complete fly-by-wire control system. Testing was conducted in both hover and forward flight and covered the complete FAA-approved envelope of the BO-105.

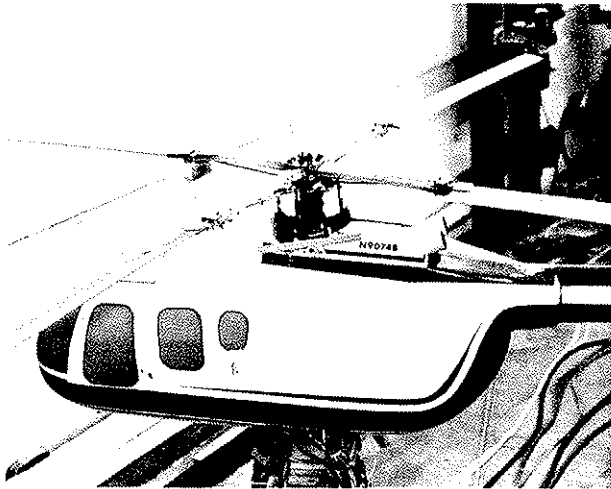


Figure 4. 1/5.86-Scale BMR/BO-105 Model in the Hover Test Cell

A typical air-resonance stability run was performed as follows: The rotor was brought up to speed and flown to a trim point, then the locking system was removed, freeing the model in pitch and roll, and the pilot stabilized the aircraft. At this point an exciter wobbled the swashplate to excite the blade lead/lag motion at its natural frequency. An oscillograph plus other computer data-reduction equipment was turned on and then the exciter was turned off. The decay in blade lead/lag motion and body pitch and roll motion was recorded. From these traces damping in the air-resonance mode was found.

The damping as a function of thrust in hover is shown in Figure 5. Damping was lowest at zero thrust and reached a maximum level of 5 percent at a thrust 1.5 times normal thrust. The typical correlation between theory and test shown in Figure 5 was very helpful in guiding configuration development. The trend of damping with thrust in hover indicates a stable configuration at normal thrust and normal rpm.

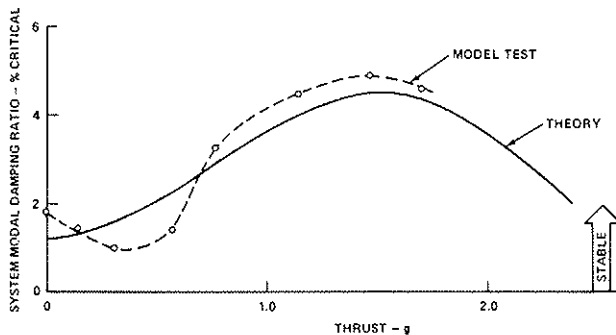


Figure 5. Air-Resonance Mode Damping Versus Thrust in Hover at Normal Rotor Speed

Damping also varies with rotor speed as indicated in Figure 6 and, in fact, an air-resonance instability was observed for rotor speeds below 330 rpm (full-scale equivalent). In the data presented in Figure 6, the collective pitch is increased as rpm is reduced, thereby maintaining a constant lg thrust regardless of rpm. The possibility of air resonance below 330 rpm was foreseen by the frequency coalescence shown in Figure 3. For the bearingless main rotor on the BO-105, this low-rpm air-resonance boundary comes about by rotor lead/lag motion coupling with body pitch motion. As noted in Figure 6, there is a reduction in damping for rotor speeds above 425 rpm, leading to a minimum in damping somewhat above 550 rpm. For the BMR/BO-105, coalescence of the rotor frequency with body roll motion did not produce an instability, even though this coalescence is shown in Figure 3.

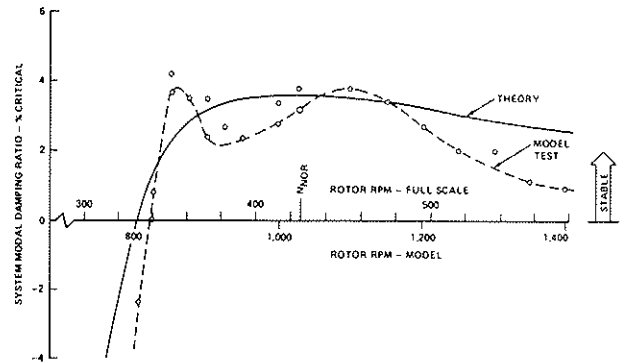


Figure 6. Air-Resonance Mode Damping Versus Rotor Speed at lg Thrust in Hover

In forward flight the configuration was always stable as shown in Figure 7. Damping versus forward speed at several load factors indicates that maneuvering, even at 135 knots, shows a satisfactory level of stability. The maximum damping, in fact, occurs in the range where power required is a maximum (or perhaps more precisely, when collective pitch is a maximum). As more and more forward-flight testing was done in the Boeing V/STOL wind tunnel, this qualitative trend that damping was first dependent on rpm and then dependent on collective pitch became evident.

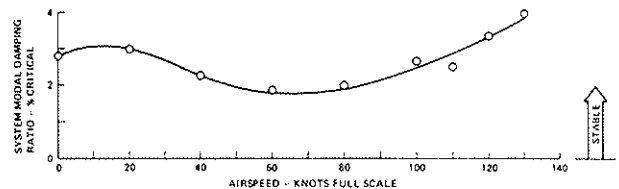


Figure 7. Typical Air-Resonance Mode Damping Versus Forward Speed at lg Thrust and Normal Rotor Speed

The dependency of damping on both rpm and collective pitch was examined more fully by testing the Froude-scaled air-resonance model in simulated climb and descent conditions at several forward speeds. An example of the test results, shown in Figure 8, indicates that damping at normal gross weight and normal rotor speed will be the least for rates of descent approaching 2,000 feet per minute. At other forward speeds the trend of damping with rate of descent was similar, but at higher damping levels.

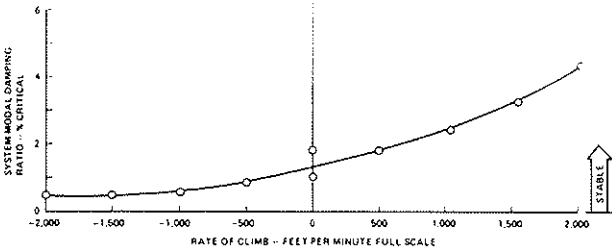


Figure 8. Typical Air-Resonance Mode Damping Versus Rate of Climb at lg Thrust, Normal Rotor Speed, and 60 Knots Full Scale

Ground Resonance

To confirm the theoretical predictions of Reference 2, a Froude-scaled ground-resonance model was constructed as shown in Figure 9. The same rotor used for air-resonance testing was transferred to this ground-resonance model. The excitation in this case will be obtained by giving a sharp jerk on a string attached to the tailboom. Damping data from an accelerometer mounted on the fuselage will then be recorded on the oscillograph.

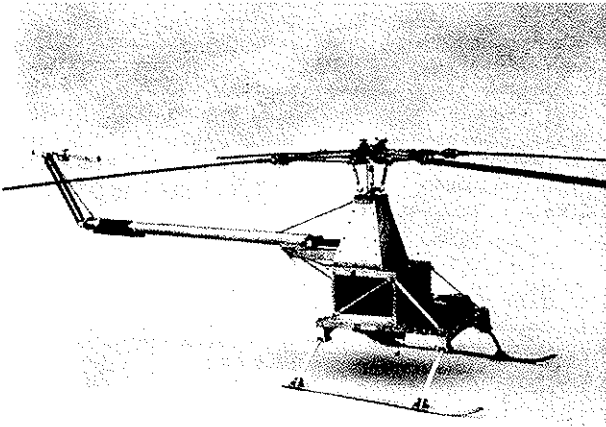


Figure 9. Ground-Resonance Model

Figure 10 shows the predicted damping levels as a function of rotor speed. The computation is for a simple overspeed of the rotor in flat pitch. These results indicate that the BMR/BO-105 is free of ground resonance within the allowable rpm ranges.

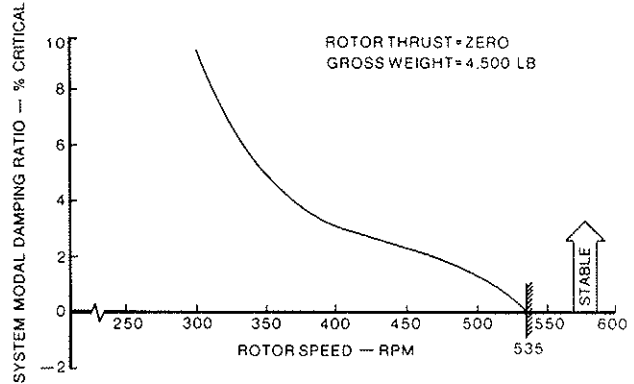


Figure 10. Final Preliminary Design is Free of Ground Resonance Over a Wide Range of Rotor Speed

Operating RPM Range

A summary of expected rpm limits is shown in Figure 11. While there are areas of rotor speed in which either air resonance or ground resonance could be encountered, Figure 11 shows that the BMR is expected to be stable within the operating range currently allowed on the BO-105, even with power off.

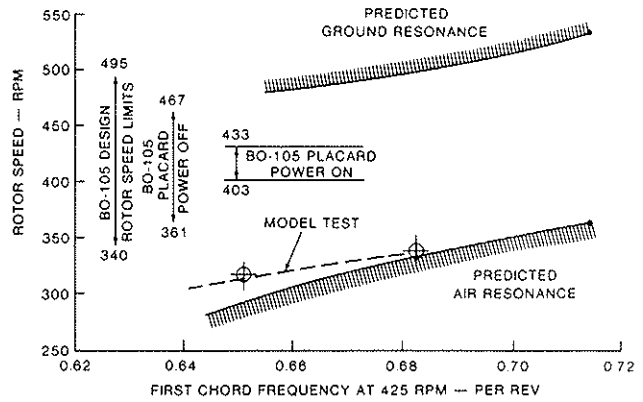


Figure 11. The BMR is Expected to be Free of Air and Ground Resonance Over a Wide Range of Rotor Speed

Structural Analysis and Test Results

The second major aspect of this program has been to design and prove that a single fiberglass element can retain the blade, provide flap stiffness and chord stiffness, and be so torsionally

soft that there is no need for pitch bearings. This major feature of the BMR has led to the following basic design criteria:

- Flight spectrum flown at 5,000-foot altitude, 100 knots, and 425 rpm for:
  - 5,150-pound gross weight and 6.3-inch forward center of gravity
  - 4,900-pound gross weight and 3.35-inch aft center of gravity
- Load factor pulled by symmetrical turn
- Yield and ultimate loading conditions of:
  - Pullup/turn at 3.5g (power on)
  - Pullup at 3.5g (power off)

From a structural point of view we have designed to a fatigue-life goal greater than 3,600 hours, assuming the flight spectrum shown in Figure 12. This flight spectrum is typical not only of today's helicopter, but also of those of the future. By careful tailoring of the fiberglass material, a preliminary design has evolved which meets or exceeds this life goal in all respects.

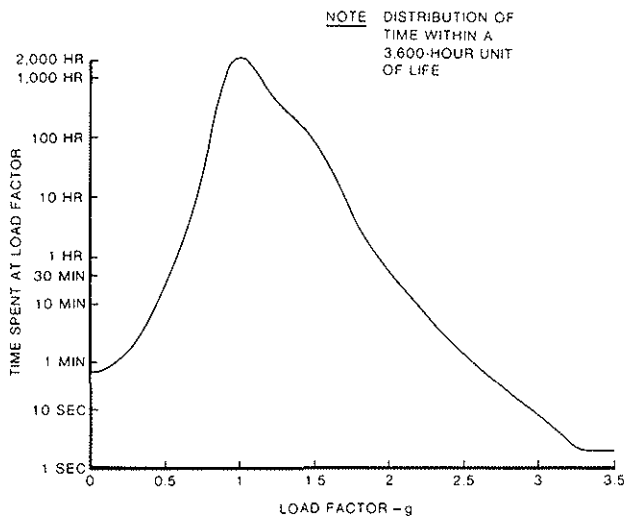


Figure 12. Design Flight Spectrum of the BMR/BO-105

A summary of the calculated lives is shown in Figure 13. The fiberglass beams have a life of 3,894 hours dictated by the cross section at station 12.4 percent. Throughout the rotor system all components have calculated lives in excess of the 3,600-hour fatigue-life goal.

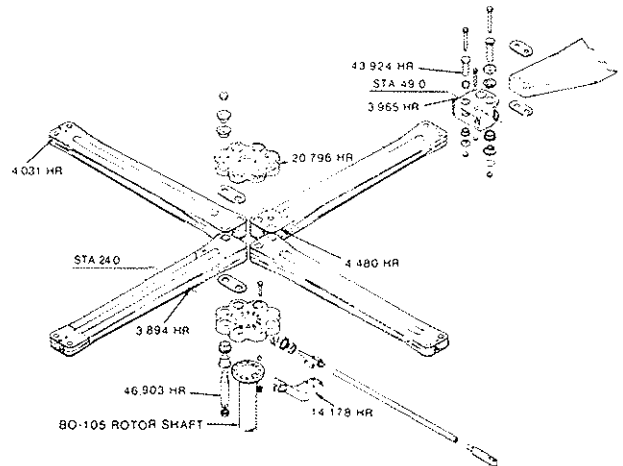


Figure 13. Fatigue Life at Key Points in the BMR System

The design conditions used in the ultimate-load analysis are as follows:

- Autorotative landing flare with 125-percent rpm, 5,150-pound gross weight, 6.3-inch forward center of gravity, 531 rpm, 2g
- Pullup/turn at 3.5g, 5,150-pound gross weight, 6.3-inch forward center of gravity, 425 rpm
- Twice maximum rotor torque, 5,150-pound gross weight, 6.3-inch forward center of gravity, 425 rpm, 2g
- Rotor startup in 45-knot wind, applied torque of twice engine maximum
- Static droop under 4g loading

The preliminary design to these ultimate conditions has insured high margins of safety at all points in the rotor system, as shown in Figure 14.

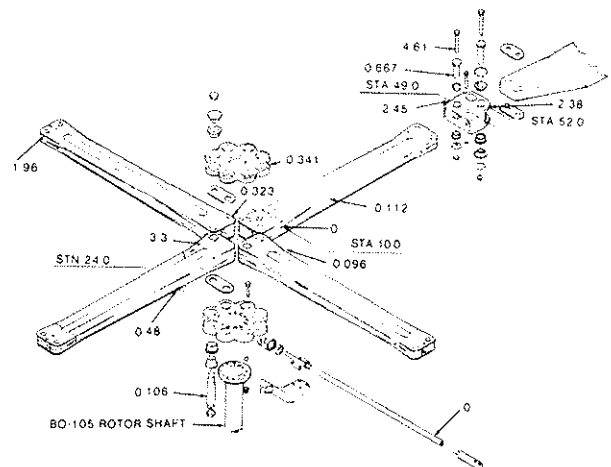


Figure 14. Ultimate Margins of Safety at Key Points in the BMR System

A unique feature of the bearingless main rotor is the twisting of the two fiberglass C-channel beams. A careful structural analysis that calculates the torsional loads which the control system must overcome was performed early in this program and then refined on the basis of several simple torsional experiments. The theory takes into account the end rigidity of a beam, the two-beam structural geometry, and the centrifugal force. The calculation and experimental confirmation of these beam torsional loads show that the BMR can be flown on the BO-105 without a major redesign of the existing control system. As shown in Figure 15, the measured torsional moment of just the beams under applied centrifugal force is 138 inch-pounds per degree; that of the aerodynamic portion of the rotor blade (accounting for both inertial and aerodynamic loads as taken from BO-105 flight-test data) is on the order of 10 inch-pounds per degree. Figure 15 shows that, with the blade attached to the beams at a pretwist angle, the sum of both beam and blade torsional loads varies with collective pitch within a usable envelope of the current BO-105 control-system capabilities.

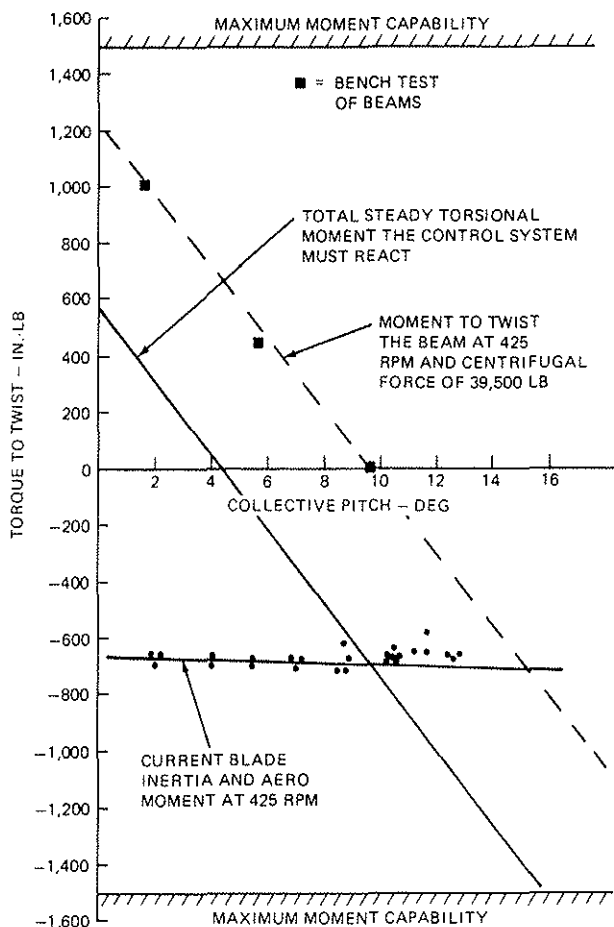


Figure 15. BMR Blade Steady Torsion Moment is Within the Capability of BO-105 Control System

Laboratory bench testing of the full-scale hardware is in progress. The loading fixture used in static and fatigue testing with the full-scale hardware mounted is shown in Figure 16. Static-deflection and load-distribution measurements, nonrotating-frequency and mode-shape tests, and fatigue testing are confirming the basic BMR design.

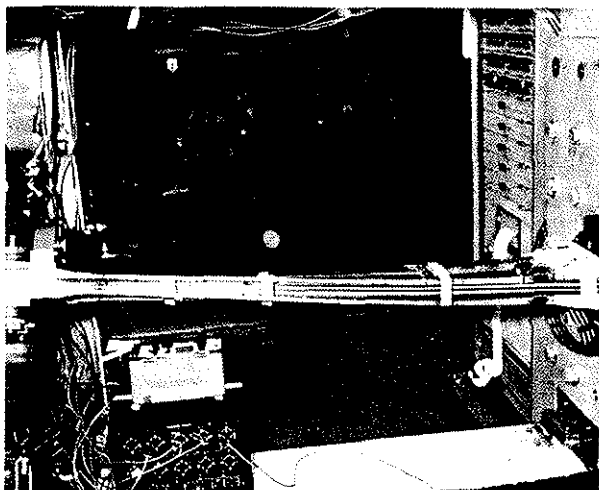


Figure 16. Fiberglass Beam in Fixture Used for Static and Fatigue Testing

#### Static Tests

Of the several static tests conducted, those to investigate torsional deflection due to applied torque are of unique interest on the BMR. The influence of centrifugal force in this regard is quite significant. As shown in Figure 17, the fiberglass beams are torsionally very soft when the simulated centrifugal force is zero. However, under simulated centrifugal force of 40,000 pounds associated with the normal 425 rpm, the torsional stiffness is increased by 2.5 times. The torsional characteristic illustrated in Figure 17 is typical of the tension-torsion packs commonly used in helicopter blade-retention systems.

The twist distributions along the fiberglass beams for the simulated-centrifugal-force cases are shown in Figure 18. This data shows that approximately 2/3 of the beam length is used to accommodate twist requirements.

Structural testing included the limit-load condition associated with a 3.5g maneuver. For this case loads were applied at the blade-to-beam joint as follows:

Simulated centrifugal force	40,000 pounds
Flap shear	7,200 pounds
Flap moment	13,747 inch-pounds

Chord shear	2,274 pounds
Chord moment	3,060 inch-pounds
Beam twist	25 degrees

key monitoring station located 24 inches out on the beams. This data shows that flap loads and simulated centrifugal force account for 75.8 percent of the total absolute strain.

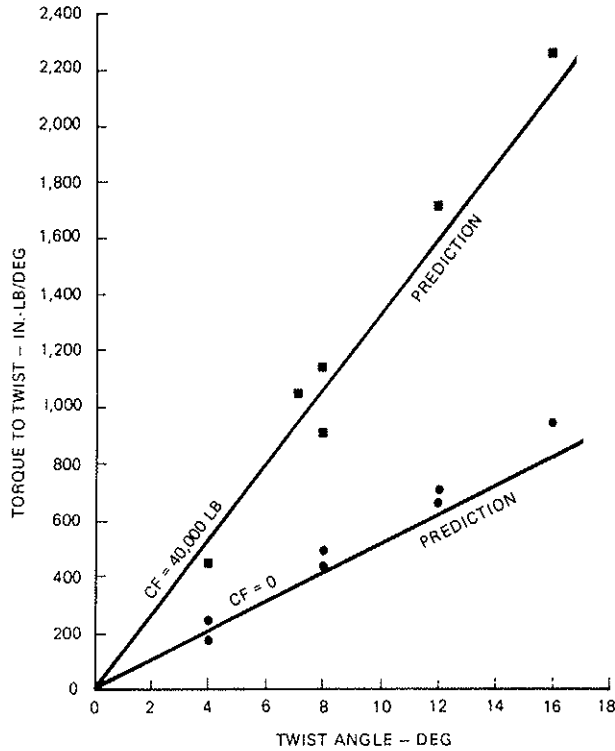


Figure 17. Torsional Characteristics of the BMR Fiberglass Beams

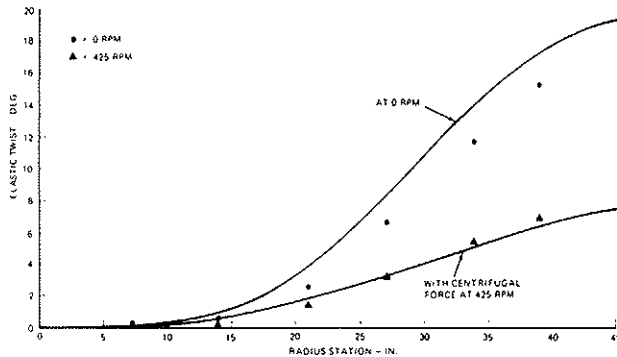


Figure 18. Elastic Twist Distribution of the BMR Beam

The measurements of absolute strain distributed radially are shown in Figure 19. The absolute strain is created by the four fundamental loads and the contribution of each load is shown in Figure 19 at the

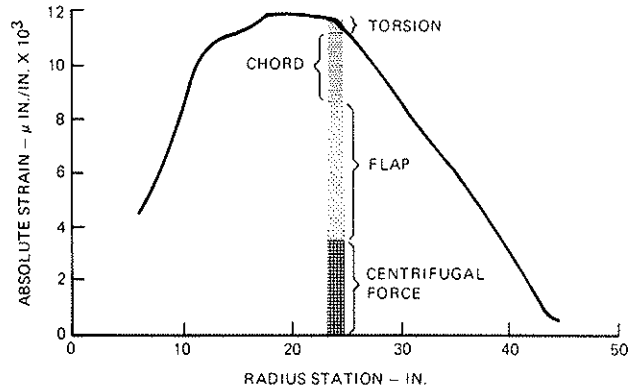


Figure 19. Limit Load Condition

#### Nonrotating-Frequency Tests

These important tests are accomplished with the complete test hardware including the blade as shown in Figure 20. Nonrotating frequencies were obtained by both bang testing and shake testing. Experimental results are in good agreement with predictions, as shown in Figure 21.

The exception to point out in Figure 21 is first chord. This frequency was predicted to be 227 cycles per minute (cpm), but was measured to be 223 cpm. If this difference of 4 cpm occurs at 425 rpm, it represents 0.012/rev. Thus, while the calculated rotating first-chord frequency is 0.739/rev at 425 rpm, we would not expect to measure data from whirl-tower testing higher than 0.727/rev. In fact, the desired and expected first-chord frequency is more on the order of 0.683/rev, as was discussed previously.

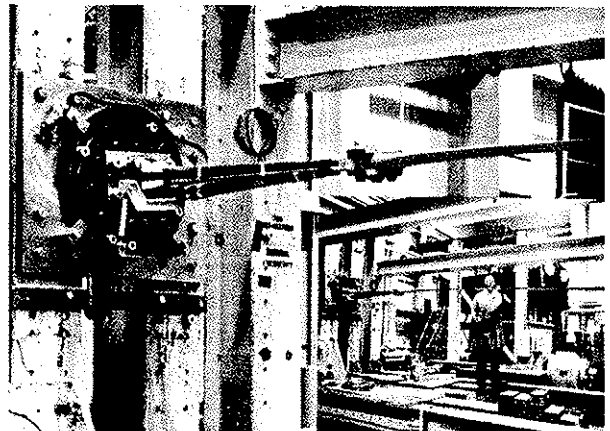


Figure 20. Laboratory Setup for Nonrotating Frequency Tests

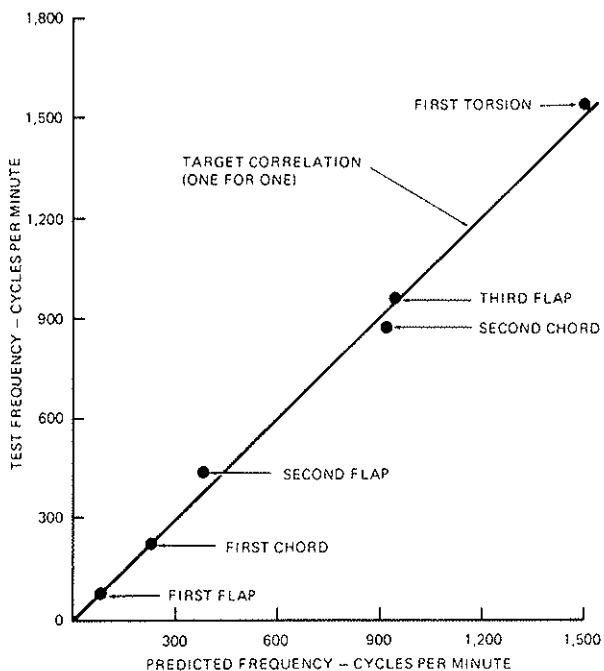


Figure 21. Correlation of Predicted and Tested Frequencies of the BMR

Fatigue Test

Fatigue testing of one fiberglass beam assembly will be completed using the test rig shown in Figure 16. The testing is being conducted to qualify at one load condition corresponding to a flight condition of:

Gross weight	5,150 pounds
Center of gravity	6.3 inches forward
Airspeed	112 knots
Altitude	5,000 feet
RPM	425
Load factor	2.0
Mast moment	60,000 inch-pounds

This flight condition is simulated with the following set of loads and deflections applied at the blade-to-beam joint:

Simulated centrifugal force	40,000 pounds
Flap shear	3,102 pounds steady, 2,648 alternating
Flap moment	5,000 inch-pounds steady, 7,284 alternating
Chord shear	760 pounds steady, 1,126 alternating

Chord moment	11,780 inch-pounds steady, 13,009 alternating
Beam twist	7 degrees steady, 9.6 alternating

At the flight condition selected and the corresponding loads and deflections, the predicted distributions of absolute strain in the critical glass fiber vary with beam radius as shown in Figure 22. For the fatigue test, absolute-strain gages are applied at several radius stations. The fatigue test will continue at the load and strain levels shown in Figure 23 for 100 hours of testing corresponding to  $3 \times 10^6$  cycles.

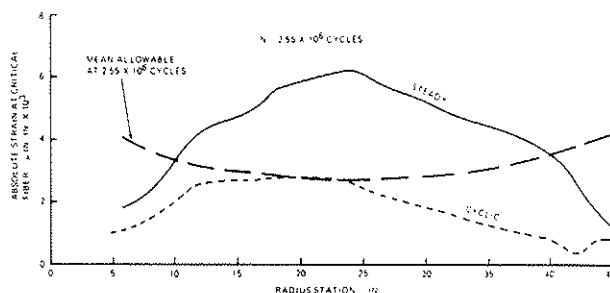


Figure 22. Predicted Strain Distribution With Applied Loads in Fatigue Test

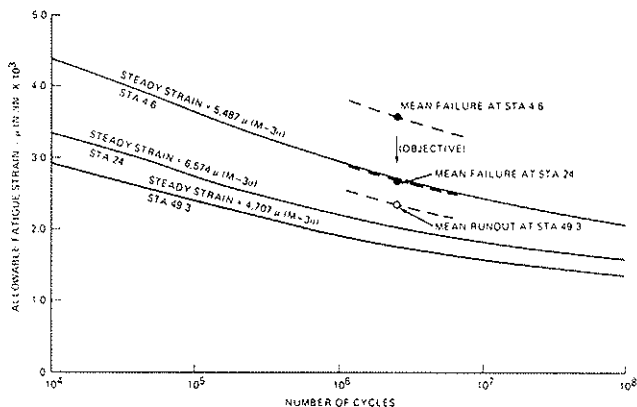


Figure 23. Fatigue Test Objectives

Next Steps in the Program

The schedule for this program is shown in Figure 24. We are presently completing our detailed design and have initiated fabrication of both whirl-tower and flight-test hardware. We expect to complete a 100-hour whirl-tower test by December of this year. The whirl-tower test will establish the rotating natural frequencies and the basic damping level of blade lead/lag motion, with the swashplate-oscillator approach. Endurance testing

will then be conducted at high thrust and normal rpm, with bending loads created by applying 2.5 degrees of cyclic pitch. With the completion of the whirl-tower test, we will move toward flight test which will begin in May 1978.

Papers giving more details of this program are planned for the American Helicopter Society Conference on Helicopter Structures Technology at the Ames Research Center, California, in November 1977.

References

1. Cardinale, Salvatore V., SOFT IN-PLANE MATCHED-STIFFNESS/FLEXURE-ROOT-BLADE ROTOR SYSTEM SUMMARY REPORT, Lockheed-California Company; USAAMRDL Technical Report 68-72, Eustis Directorate, U.S. Army Air Mobility Research and Development Laboratory, Fort Eustis, Virginia, August 1969.
2. FLIGHT EVALUATION OF LOADS AND STABILITY CHARACTERISTICS OF A BEARINGLESS MAIN ROTOR (BMR), Contract DAAJ02-76-C-0029, Eustis Directorate, U.S. Army Air Mobility Research and Development Laboratory, Fort Eustis, Virginia, June 1976.

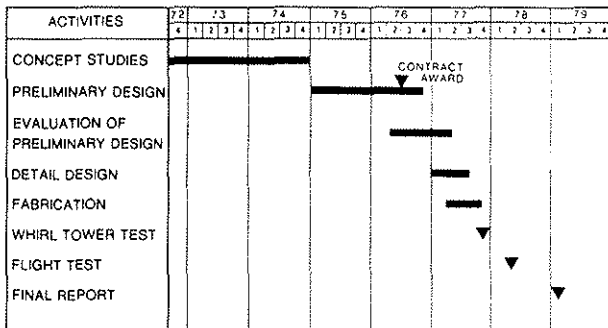


Figure 24. Schedule for the Bearingless Main Rotor Program